IISRC International Industrial Scientific Research Corporation
International Conference on Industrial Scientific Research Engineering
www.worldconferences.org

A Hybrid Wind-Photovoltaic System with Multi-input CUK and SEPIC Rectifier Topology

N. THRIVIKRAMARAJU[1], K. KALYANKUMAR[2]
[1]PG Scholar in the Department of Electrical Engineering, K.S.R.M College of Engineering, Kadapa, A.P-INDIA, Email: vikramreacal@gmail.com.
[2]Asst Prof in the Department of Electrical Engineering, K.S.R.M College of Engineering, Kadapa, A.P-INDIA, Email: kalyankumark13@gmail.com.

Abstract: With increasing concern of global warming and the depletion of fossil fuel reserves, many are looking at sustainable energy solutions to preserve the earth for the future generations. This paper presents a new system configuration of the front-end rectifier stage for a hybrid wind/photovoltaic energy system. This configuration allows the two sources to supply the load separately or simultaneously depending on the availability of the energy sources. The inherent nature of this CUK-SEPIC fused converter, additional input filters are not necessary to filter out high frequency harmonics. Harmonic content is detrimental for the generator lifespan, heating issues, and efficiency. The fused multi- input rectifier stage also allows Maximum Power Point Tracking (MPPT) to be used to extract maximum power from the wind and sun when it is available. An adaptive MPPT algorithm is used for the wind system and a standard perturb and observe method is used for the PV system. Operational analysis of the proposed system is discussed in this paper. Simulation results are given to highlight the merits of the proposed Model.

Keywords: CUK, Hill Climb Search (HCS), MPPT, SEPIC, Tip Speed Ratio (TSR).

I. INTRODUCTION

Environmentally friendly solutions are becoming more prominent than ever as a result of concern regarding the state of our deteriorating planet. Other than hydro power, wind and photovoltaic energy holds the most potential to meet our energy demands. Alone, wind energy is capable of supplying large amounts of power but its presence is highly unpredictable as it can be here one moment and gone in another. Similarly, solar energy is present throughout the day but the solar irradiation levels vary due to sun intensity and unpredictable shadows cast by clouds, birds, trees, etc. The common inherent drawback of wind and photovoltaic systems are their intermittent natures that make them unreliable. However, by combining these two intermittent sources and by incorporating maximum power point tracking (MPPT) algorithms, the system's power transfer efficiency and reliability can be improved significantly. When a source is unavailable or insufficient in meeting the load demands, the other energy source can compensate for the difference. Several hybrid wind and PV power systems with MPPT control have been proposed and discussed in works [1]-[5]. Most of the systems in literature use a separate DC/DC boost converter connected in parallel in the rectifier stage as shown in Figure 1 to perform the MPPT control for each of the renewable energy power sources [1]-[4].

In this paper, an alternative multi-input rectifier structure is proposed for hybrid wind/solar energy systems. The proposed design is a fusion of the CUK and SEPIC converters. The features of the proposed topology are: 1) the inherent nature of these two converters eliminates the need for separate input filters for PFC [7]-[8]. 2) It can support step up/down operations for each renewable source (can support wide ranges of PV and wind input). 3) MPPT can be realized for each source. 4) Individual and simultaneous operation is supported.

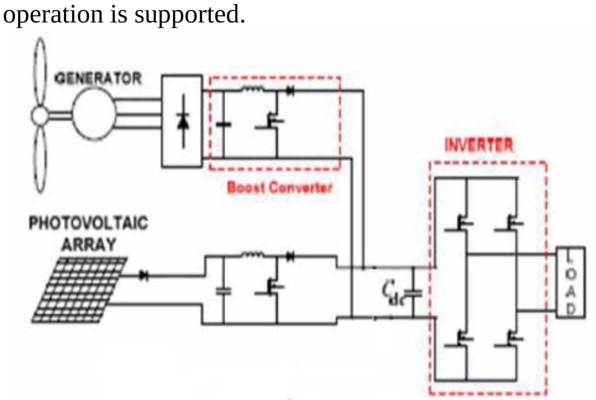

Figure1. Hybrid system with multi-connected boost converter

II. PROPOSED MULTI-INPUT RECTIFIER STAGE

A system diagram of the proposed rectifier stage of a hybrid energy system is shown in Figure 2, where one of the inputs is connected to the output of the PV array and the other input connected to the output of a generator. This configuration allows each converter to operate normally individually in the event that one source is unavailable. In the case of when only the wind source is available, D1 turns off and D2 turns on; the proposed circuit becomes a SEPIC converter and the input to output voltage relationship is given by (1). On the other hand, if only the PV source is available, then D2 turns off and D1 will always be on and the circuit becomes a CUK converter as shown in Figure 4. The input to output voltage relationship is given by (2).

$$Vdc / Vw = d2 / (1-d2) \quad (1)$$
$$Vdc / Vpv = d1 / (1-d1) \quad (2)$$

Figure3 illustrates the various switching states of the proposed converter. If the turn on duration of M1 is longer than M2, then the switching states will be state I, II, IV. Similarly, the switching states will be state I, III, IV if the switch conduction periods are vice versa. To provide a better explanation, the inductor current waveforms of each switching state are given as follows assuming that d2 > d1; hence only states I, III, IV are discussed in this example. In the following, Ii, PV is the average input current from the PV source; Ii, W is the RMS input current after the rectifier (wind case); and Idc is the average system output current. The key waveforms that illustrate the switching states in this example are shown in Figure4. The mathematical expression that relates the total output voltage and the two input sources will be illustrated in the next section.

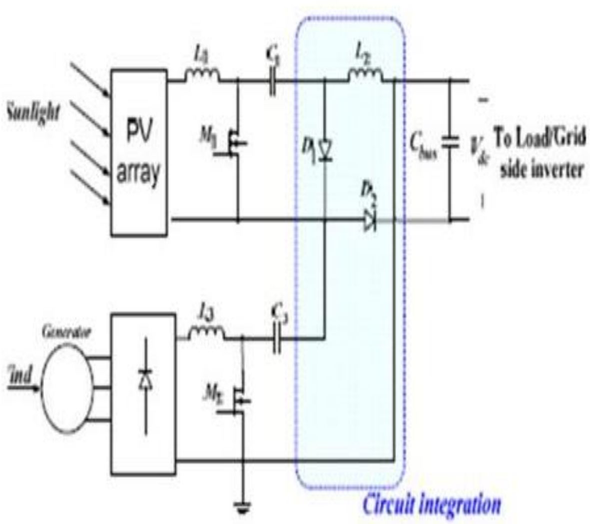

Figure2. Proposed Rectifier stage for a Hybrid Wind/PV System

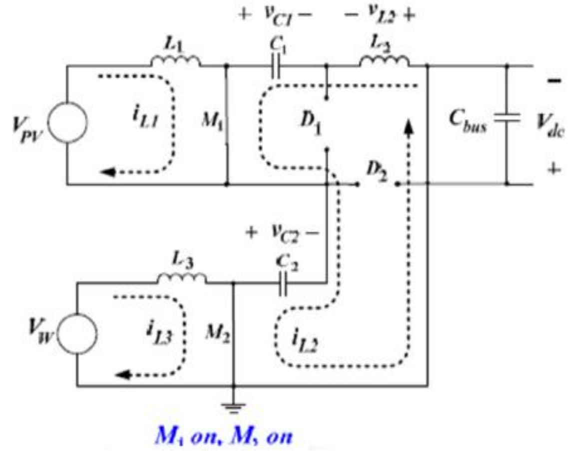

$$i_{L1} = I_{i,PV} + \frac{V_{PV}}{L_1} t$$

$$i_{L2} = I_{dc} + \left(\frac{v_{c1} + v_{c2}}{L_2} \right) t$$

$$i_{L3} = I_{i,W} + \frac{V_W}{L_3} t$$

State I

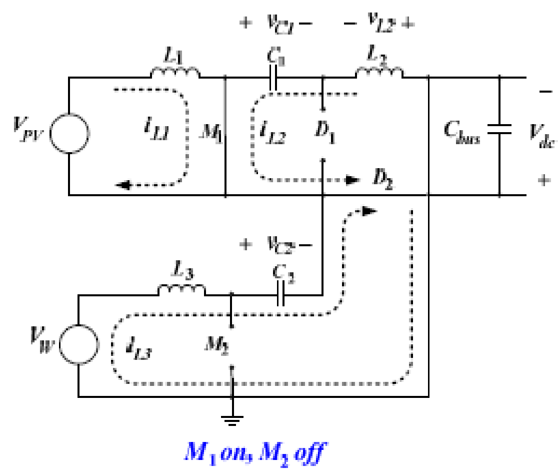

State II

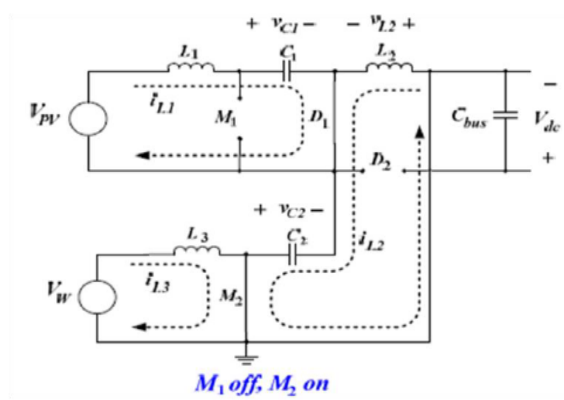

$$i_{L1} = I_{i,PV} + \left(\frac{V_{PV} - v_{c1}}{L_1} \right) t$$

$$i_{L2} = I_{dc} + \frac{v_{c2}}{L_2} t$$

$$i_{L3} = I_{i,W} + \frac{V_W}{L_3} t$$

State III

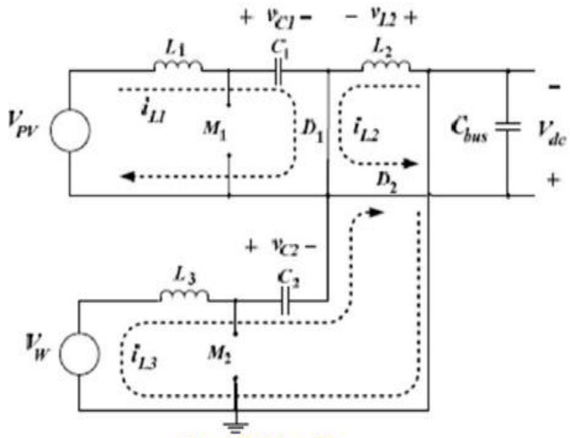

M_1 off, M_2 off

$$i_{L1} = I_{i,PV} + \left(\frac{V_{PV} - v_{c1}}{L_1}\right) t$$

$$i_{L2} = I_{dc} - \frac{V_{dc}}{L_2} t$$

$$i_{L3} = I_{i,W} + \left(\frac{V_W - v_{c2} - V_{dc}}{L_3}\right) t$$

State IV

Figure3. State (I-IV): Switching States within a switching Cycle

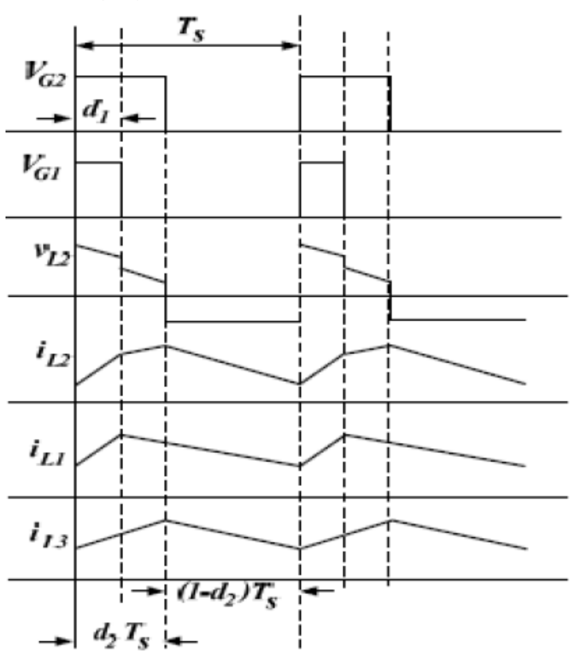

Figure4. Proposed circuit inductor waveforms

III. ANALYSIS OF PROPOSED CIRCUIT

To find an expression for the output DC bus voltage, Vdc, the volt-balance of the output inductor, L2, is examined according to Figure 4 with d2 > d1. Since the net change in the voltage of L2 is zero, applying volt-balance to L2 results in (3). The expression that relates the average output DC voltage (Vdc) to the capacitor voltages (vc1 and vc2) is then obtained as shown in (4), where vc1 and vc2 can then be obtained by applying volt-balance to L1 and L3 [9]. The final expression that relates the average output voltage and the two input sources (VW and VPV) is then given by (5). It is observed that Vdc is simply the sum of the two output voltages of the Cuk and SEPIC converter. This further implies that Vdc can be controlled by d1 and d2 individually or simultaneously.

$$(Vc1 + Vc2)d1Ts + (Vc2)(d2-d1)Ts + (1-d2)(-Vdc)Ts = 0 \quad (3)$$

$$Vdc = (d1/(1-d2))Vc1 + (d2/(1-d2))Vc2 \quad (4)$$

$$Vdc = (d1/(1-d1))VPV + (d2/(1-d2))Vw \quad (5)$$

The switches voltage and current characteristics are also provided in this section. The voltage stress is given by (6) and (7) respectively. As for the current stress, it is observed from Figure 4 that the peak current always occurs at the end of the on-time of the MOSFET. Both the Cuk and SEPIC MOSFET current consists of both the input current and the capacitors (C1 or C2) current. The peak current stress of M1 and M2 are given by (8) and (10) respectively. Leq1 and Leq2, given by (9) and (11), represent the equivalent inductance of Cuk and SEPIC converter respectively. The PV output current, which is also equal to the average input current of the Cuk converter, is given in (12). It can be observed that the average inductor current is a function of its respective duty cycle (d1). Therefore by adjusting the respective duty cycles for each energy source, maximum power point tracking can be achieved.

$$Vds1 = VPV\,(1 + (d1/(1-d1))) \quad (6)$$

$$Vds2 = Vw\,(1 + (d2/(1-d2))) \quad (7)$$

$$ids1.pk = Ii.PV + Idc.avg + (VPVd1Ts / 2Leq1) \quad (8)$$

$$Leq1 = (L1L2/(L1+L2)) \quad (9)$$

$$ids2.pk = Ii.w + Idc.avg + (Vwd2Ts / 2Leq2) \quad (10)$$

$$Leq2 = (L3L2/(L3+L2)) \quad (11)$$

$$Ii.PV = (P0 / Vdc)(d1 / (1-d1)) \quad (12)$$

IV. MPPT CONTROL OF PROPOSED CIRCUIT

A common inherent drawback of wind and PV systems is the intermittent nature of their energy sources. Wind energy is capable of supplying large amounts of power but its presence is highly unpredictable as it can be here one moment and gone in another. Solar energy is present throughout the day, but the solar irradiation levels vary due to sun intensity and unpredictable shadows cast by clouds, birds, trees, etc. These drawbacks tend to make these renewable systems inefficient. However, by incorporating maximum power point tracking (MPPT) algorithms, the systems' power transfer efficiency can be improved significantly. To describe a wind turbine's power characteristic, equation (13) describes the mechanical power that is generated by the wind [6].

$$Pm= 0.5\rho ACp\ (\lambda, \beta)\ vw3 \qquad (13)$$

Where
ρ = air density,
A = rotor swept area,
Cp(λ, β) = power coefficient function
λ =tip speed ratio,
β = pitch angle,
vw = wind speed.

The power coefficient (Cp) is a nonlinear function that represents the efficiency of the wind turbine to convert wind energy into mechanical energy. It is dependent on two variables, the tip speed ratio (TSR) and the pitch angle. The TSR, λ, refers to a ratio of the turbine angular speed over the wind speed. The mathematical representation of the TSR is given by (14) [10]. The pitch angle, β, refers to the angle in which the turbine blades are aligned with respect to its longitudinal axis.

$$\lambda = R\ \omega b\ /\ Vw \qquad (14)$$

Where
R = turbine radius,
ωb = angular rotational speed.

Figure5 and 6 are illustrations of a power coefficient curve and power curve for a typical fixed pitch (β =0) horizontal axis wind turbine. It can be seen from figure 5 and 6 that the power curves for each wind speed has a shape similar to that of the power coefficient curve. Because the TSR is a ratio between the turbine rotational speed and the wind speed, it follows that each wind speed would have a different corresponding optimal rotational speed that gives the optimal TSR. For each turbine there is an optimal TSR value that corresponds to a maximum value of the power coefficient (Cp,max) and therefore the maximum power. Therefore by controlling rotational speed, (by means of adjusting the electrical loading of the turbine generator) maximum power can be obtained for different wind speeds

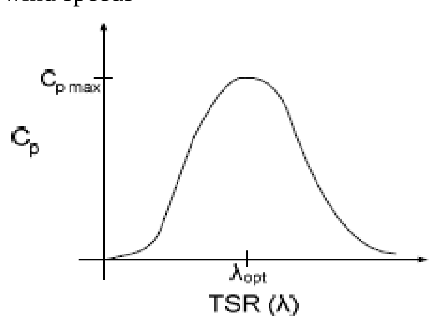

Figure5. Power Coefficient Curve for a typical turbine

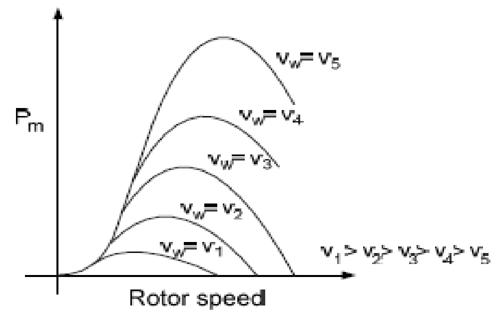

Figure6: Power Curves for a typical wind turbine

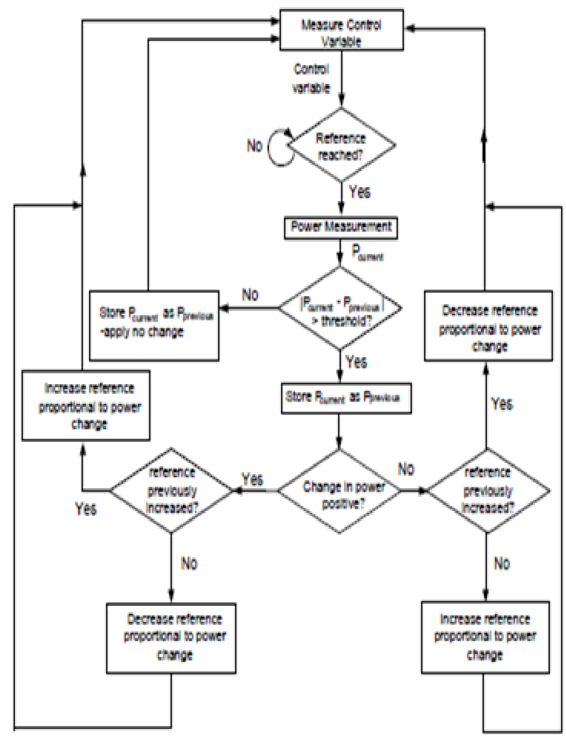

Figure7. Algorithm Implementation

A solar cell is comprised of a P-N junction semiconductor that produces currents via the photovoltaic effect. PV arrays are constructed by placing numerous solar cells connected in series and in parallel [5]. A PV cell is a diode of a large-area forward bias with a photo voltage and the equivalent circuit is shown by Figure 7 [11]. The current- voltage characteristic of a solar cell is derived in [12] and [13] as follows:

$$I = I_{ph} - I_D \qquad (15)$$

$$I = I_{ph} - I_0[(\exp(q(V+R_S I)/AK_B T))-1]-((V+R_S I)/R_{sh}) \qquad (16)$$

Where
I_{ph} = photocurrent,
I_D = diode current,

I_0 = saturation current, A = ideality factor,
q = electronic charge 1.6x10-9,
k_B = Boltzmann's gas constant (1.38x10-23), T = cell temperature,
R_s = series resistance, R_{sh} = shunt resistance, I = cell current,
V = cell voltage

V. SIMULATION RESULTS

In this section, simulation results from PSIM 8.0.7 is given to verify that the proposed multi-input rectifier stage can support individual as well as simultaneous operation. The specifications for the design example are given in TABLEI.

TABLE I. Design Specifications

Output power (W)	3kW
Output voltage	500V
Switching frequency	20kHz

A. Simulation diagram of hybrid wind solar energy system

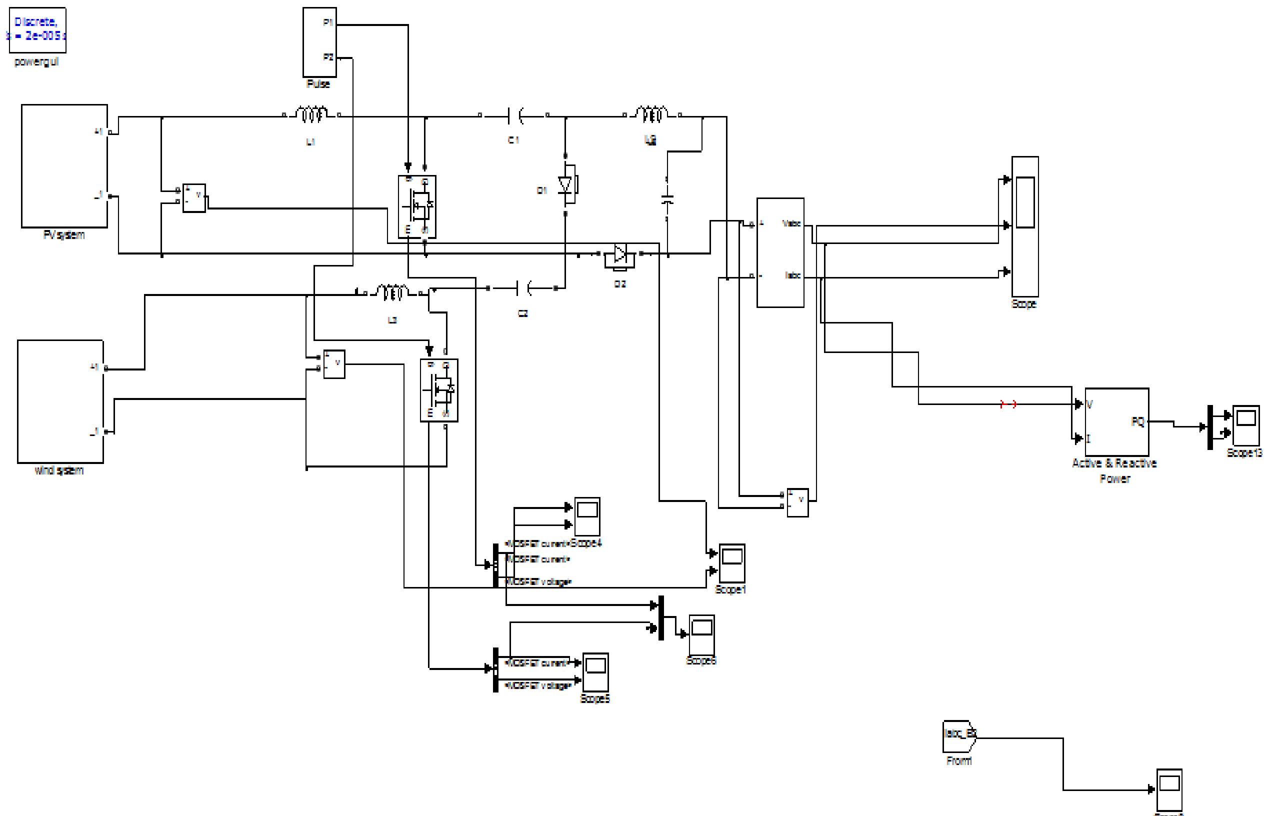

Figure8. Simulink Model

B. Simulation Results

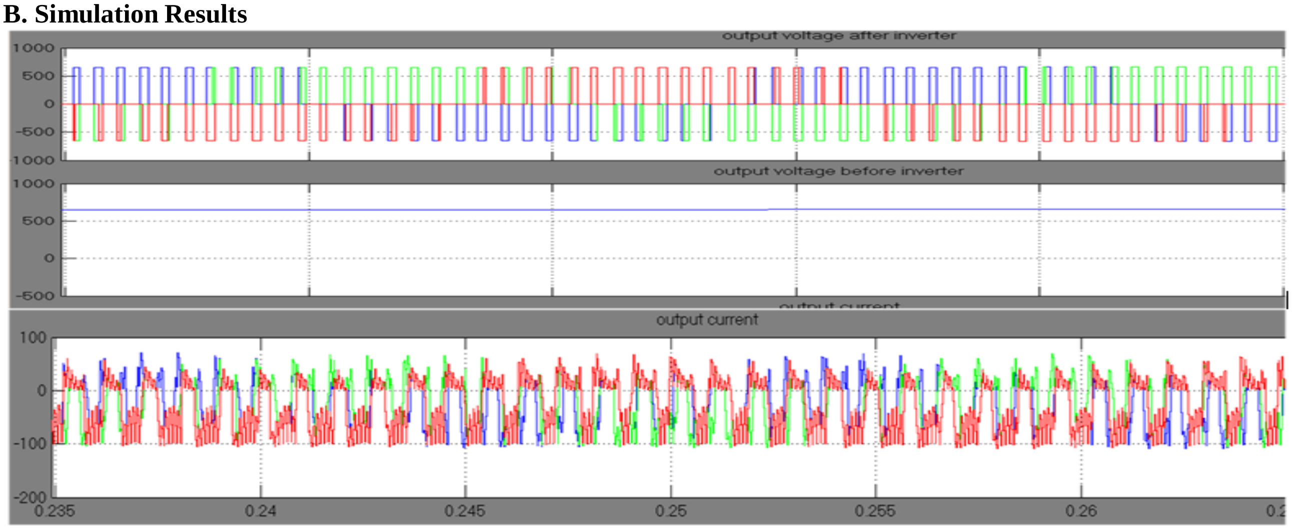

Figure9. Hybrid Output voltage before and after inverter and inverter current of wind & PV

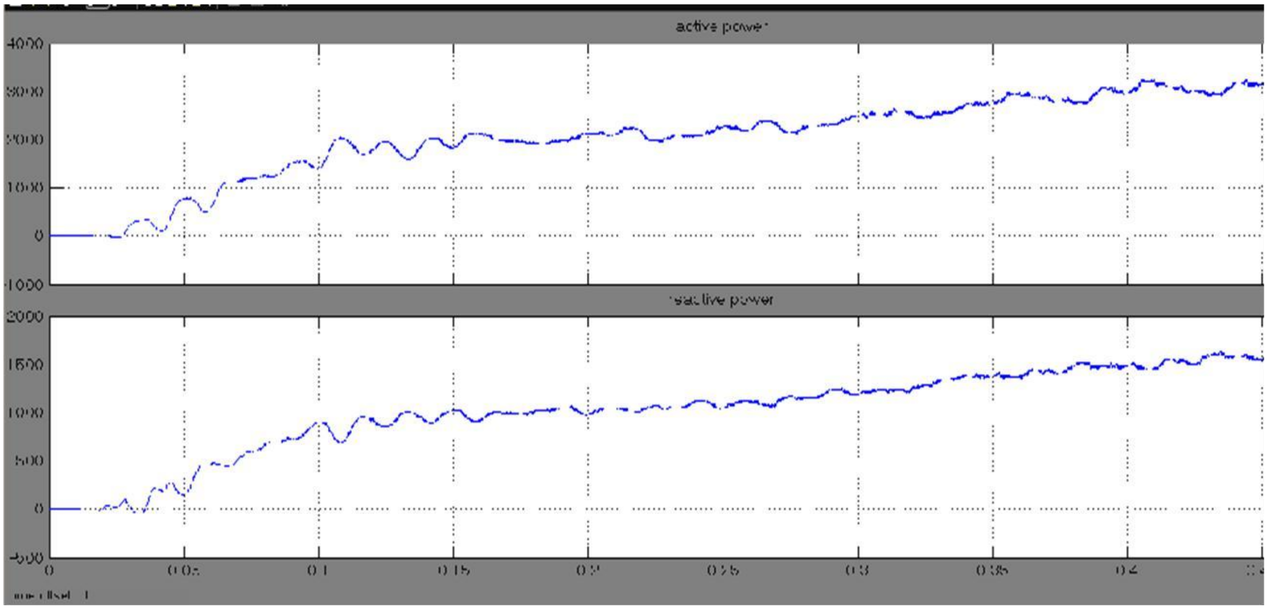

Figure10. Active & reactive power of Hybrid system

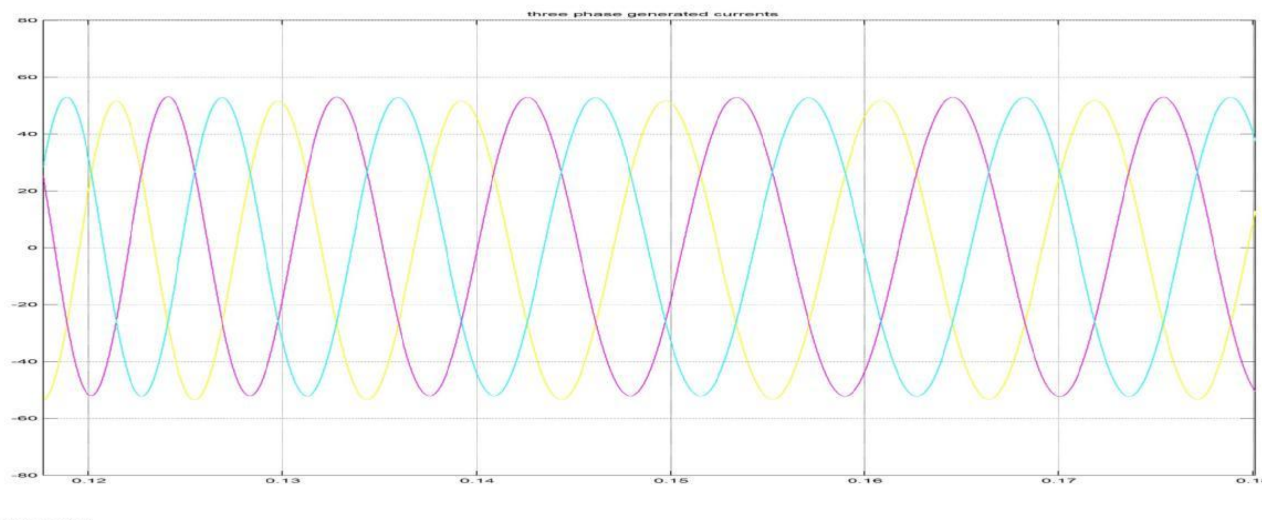

Figure11. Three Phase Generated Currents

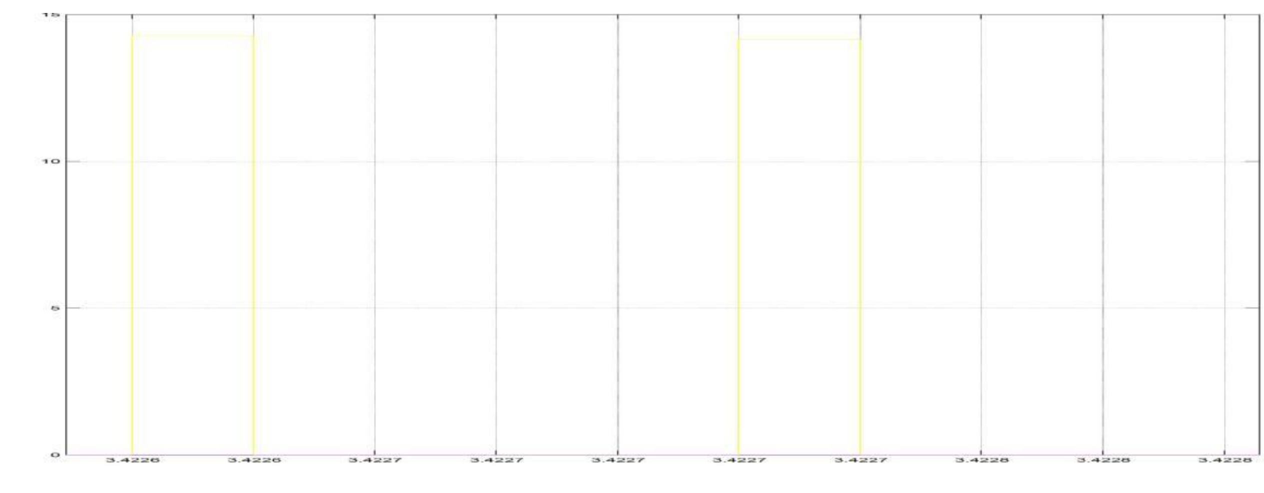

Figure12. Switching Currents

VI. CONCLUSION

In this paper a new multi-input Cuk-SEPIC rectifier stage for hybrid wind/solar energy systems has been presented. The features of this circuit are: 1) additional input filters are not necessary to filter out high frequency harmonics; 2) both renewable sources can be stepped up/down (supports wide ranges of PV and wind input); 3) MPPT can be realized for each source; 4) individual and simultaneous operation is supported. Simulation results have been presented to verify the features of the proposed topology.

VII. REFERENCES

[1] S.K. Kim, J.H Jeon, C.H. Cho, J.B. Ahn, and S.H. Kwon, "Dynamic Modeling and Control of a Grid-Connected Hybrid Generation System with Versatile Power Transfer," IEEE Transactions on Industrial Electronics, vol. 55, pp. 1677-1688, April 2008.

[2] D. Das, R. Esmaili, L. Xu, D. Nichols, "An Optimal Design of a Grid Connected Hybrid Wind/Photovoltaic/ Fuel Cell System for Distributed Energy Production," in Proc. IEEE Industrial Electronics Conference, pp. 2499-2504, Nov. 2005.

[3] N. A. Ahmed, M. Miyatake, and A. K. Al-Othman, "Power fluctuations suppression of stand-alone hybrid generation combining solar photovoltaic/wind turbine and fuel cell systems," in Proc. Of Energy Conversion and Management, Vol. 49, pp. 2711-2719, October 2008.

[4] S. Jain, and V. Agarwal, "An Integrated Hybrid Power Supply for Distributed Generation Applications Fed by Nonconventional Energy Sources," IEEE Transactions on Energy Conversion, vol. 23, June 2008.

[5] Y.M. Chen, Y.C. Liu, S.C. Hung, and C.S. Cheng, "Multi-Input Inverter for Grid-Connected Hybrid PV/Wind Power System," IEEE Transactions on Power Electronics, vol. 22, May 2007.

[6] Dos Reis, F.S., Tan, K. and Islam, S., "Using PFC for harmonic mitigation in wind turbine energy conversion systems" in Proc. of the IECON 2004 Conference, pp.3100- 3105, Nov. 2004.

[7] R. W. Erickson, "Some Topologies of High Quality Rectifiers" in the Proc. of the First International Conference on Energy, Power, and Motion Control, May 1997.

[8] D. S. L. Simonetti, J. Sebasti´an, and J. Uceda, "The Discontinuous Conduction Mode Sepic and ´ Cuk Power Factor Preregulators: Analysis and Design" IEEE Trans. On Industrial Electronics, vol. 44, no. 5, 1997.

[9] N. Mohan, T. Undeland, and W Robbins, "Power Electronics: Converters, Applications, and Design," John Wiley & Sons, Inc., 2003.

[10] J. Marques, H. Pinheiro, H. Grundling, J. Pinheiro, and H. Hey, "A Survey on Variable-Speed Wind Turbine System," Proceedings of Brazilian Conference of Electronics of Power, vol. 1, pp. 732-738, 2003.

[11] F. Lassier and T. G. Ang, "Photovoltaic Engineering Handbook" 1990.

[12] Global Wind Energy Council (GWEC), "Global wind 2008 report," June 2009.

[13] L. Pang, H. Wang, Y. Li, J. Wang, and Z. Wang, "Analysis of Photovoltaic Charging System Based on MPPT," Proceedings of Pacific-Asia Workshop on Computational Intelligence and Industrial Application 2008 (PACIIA '08), Dec 2008, pp. 498-501.